Do we really know how to derive the basic PNe parameters?

Denise R. Gonçalves

IAG, Universidade de São Paulo, Rua do Matão 1226, 05508-900, São Paulo, Brazil

Abstract. How well do we know the physical/chemical properties of PNe? 1D (CLOUDY) and 3D (MOCASSIN) photoionisation codes are used in this contribution to model the PNe K 4-47 and NGC 7009 as an attempt to question whether or not the high Te (higher than 21,000K) of the K 4-47's core and the N overabundance of the outer knots in NGC 7009 are real.

These are very basic parameters, obtained for Galactic PNe, e.g. nearby objects, even though with large uncertainties. Based on the comparison of the modelling with, mainly, optical images and long-slit spectroscopic data, it is suggested here that K 4-47 high Te can be explained if its core is composed of a very dense and small inner region – that matches the radio measurements– and a lower density outer core –matching the optical observations. This approach can account for the strong auroral emission lines [OIII]4363Å and [NII]5755Å observed, and so for the high temperatures. This teaches us that the assumption of a homogeneous distribution of the gas is completely wrong for the core of such PN.

In the case of NGC 7009 a simple 3D model that reproduces the observed geometry of this nebula is constructed. The aim of this modelling was to explore the possibility that the enhanced [NII] emission observed in the outer knots may be due to ionisation effects instead to a local N overabundance. Here it is discussed the model that can best reproduce the observations employing a *homogeneous* set of abundances throughout the nebula, not only for *nitrogen* but also for all the other elements considered.

Keywords: <Enter Keywords here>
PACS: <Replace this text with PACS numbers; choose from this list: `http://www.aip..org/pacs/index.html`>

AN INTRODUCTION TO K 4-47 AND NGC 7009

These two PNe are similar in that both have pairs of low-ionisation knots and jets, the former being known as FLIERS (fast, low-ionisation emission regions, Balick et al. 1993). Because the fact that K 4-47 and NGC 7009 most appealing features are those of small-scales –knots and jets– in spite of their large-scale structures –rim, shell and halo– spatially resolved analysis becomes mandatory for describing them properly.

A couple of years ago we (Gonçalves et al. 2003, 2004) published the analysis of these PNe, based on their spatially resolved long-slit spectroscopic data –namely physical, chemical and excitation properties– as part of a wider project aimed at the study of these properties for a large sample of PNe that are known to possess small-scale low-ionisation structures, LIS (see Gonçalves 2003 for a review on LIS of PNe).

As it is shown in Figure 1, K 4-47 is a compact PN, composed by a small, high ionisation nebular core and a pair of low-ionisation, high-velocity knots, connected to the core by a much fainter low-ionisation lane (Corradi et al. 2000). Gonçalves et al. (2001) have proposed that the low-ionisation lanes and knots of K 4-47 are genuine jets, and that their morphological and kinematic properties can be explained if the jets and knots were formed by accretion disks, attaining velocities of several hundred kilometers per second. These highly supersonic veloci-
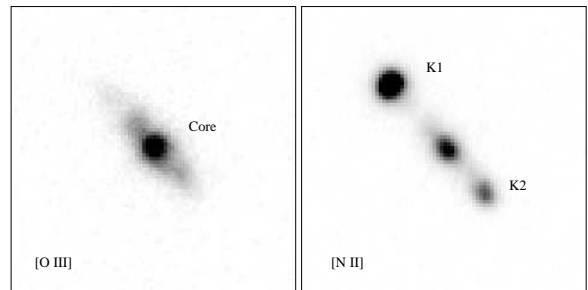
FIGURE 1. NOT [O III] and [N II] images of K 4-47, putting in evidence the prominent [N II] pair of knots and the [O III] prominent core. The sizes of the boxes are 15×15 arcsec.

ties imply that the resulting LIS are likely to be shock-excited. This is a poorly studied PN, with statistical distances ranging from 8.5 kpc (Cahn, Kaler & Stanghellini 1992) to 26 kpc (van de Steene & Zijlstra 1994). Corradi et al. (2000) restricted this range to 3 - 7 kpc, assuming that the object participates in the ordered rotation of the disk of the Galaxy. Tajitsu & Tamura (1998) estimated a distance of 5.9 kpc using the integrated *IRAS* fluxes under the assumption of constant dust mass for all PNe. Lacking of better information, we adopt the latter value in this work. Lumsden et al. (2001) mapped the H_2 emission from K 4-47 finding that it is excited by shocks. The object also appears in the 6 cm VLA radio survey of Aaquist & Kwok (1990) showing a very compact radio core, with a diameter of 0.25 arcsec, and one of the
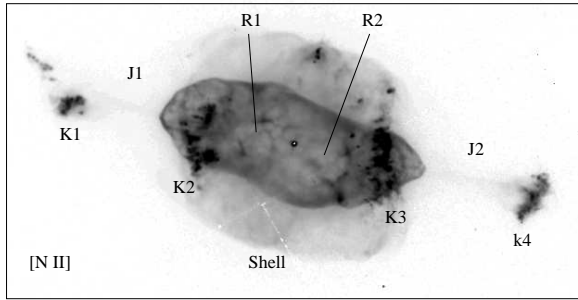
FIGURE 2. HST [N II] image of NGC 7009, in logarithmic scale. Labels mark the positions of the outer (K1, K4) and inner (K2, K3) pair of knots, the pair of jets (J1, J2), the rim (R1, R2) and the shell. The size of the box is 65×32 arcsec.

largest brightness temperatures (T_b=8,700 K) found in PNe. So far, the properties (luminosity and temperature) of its central star are not known.

As for the "Saturn Nebula", NGC 7009, it comprises a bright elliptical rim and a tenuous halo. Its small-scale structures include a pair of jets and two pairs of low-ionisation knots (see Figure 2). High-excitation lines dominate the inner regions along the minor axis, while emission from low-ionisation species is enhanced at the extremities of the major axis. NGC 7009 was classified as an oxygen-rich PN (Hyung & Aller 1995), with an O/C ratio exceeding 1, and anomalous N, O, and C abundances (Balick et al. 1994, Hyung & Aller 1995). Its central star is an H-rich O-type star, with an effective temperature of 82,000 K (Méndez et al. 1992). Reay & Atherton (1985) showed that the outer knots are expanding near the plane of the sky at highly supersonic velocities, and that the inclination of the inner (caps) and outer (ansae) knots, with respect to the line of sight, are $i \cong 51°$ and $i \cong 84°$, respectively. More recently, Fernández et al. (2004) have measured the proper motion and kinematics of the ansae in NGC 7009, obtaining V_{exp} = 114 ± 32 km s^{-1}, for a distance of $\sim 0.86 \pm 0.34$ kpc.

EMPIRICAL PHYSICAL AND CHEMICAL PROPERTIES

As described in Gonçalves et al. (2003 and 2004), the observations used in the present discussion include [O III] and [N II] images of both PNe, as well as long-slit, intermediate dispersion spectra taken along the PNe major axes (P.A. are 41° and 79°, for K 4-47 and NGC 7009, respectively).

The physical parameters for these PNe were obtained from the following line ratios:

1. [S II] 6717Å/6731Å and [Cl III] 5517Å/5537Å, for electron densities;

2. [O III] (4959Å+5007Å)/4363Å, [N II] (6548Å+ 6583Å)/5755Å and [S II] (6716Å+6731Å)/(4069Å+ 4076Å), for electron temperatures.

The total abundances for the different structures in these PNe were derived from an empirical analysis that uses the ionisation correction factors (*icf*) to account for the unseen ions (e.g. Kingsburgh & Barlow, 1994). Results obtained with the *icf* method can be somewhat uncertain, particularly when they are applied to spatially resolved long-slit spectra (Alexander & Balick 1997), as it is the case in the present work.

K 4-47:

Electron densities and temperatures of K 4-47 are listed in Table 1. Both knots are denser than the core (1,900 cm^{-3}) by factors of 2.4 and 1.2 for K_1 and K_2, respectively. T_e[O III], appropriate to zones of medium to high excitation, and T_e[N II] characteristic of low-excitation regions are also shown, and in two cases they are only lower limits. Note that temperatures of K 4-47 are remarkably higher than the typical values for PNe (around 10^4 K). In addition to these high T_e, diagnostic diagrams (not shown here) also suggest that shock excitation play an important role in the high-velocity knots of this PN, but not in its core.

TABLE 1. Physical parameters of K 4-47

N_e (cm^{-3}) T_e (K)	K1	Core	K2	Whole nebula
N_e[SII]	4,600	1,900	2,400	2,800
T_e[OIII]	≥21,000	19,300	16,100	19,300
T_e[NII]	18,900	≥21,000	16,950	20,600

Keeping in mind that the Core seems to be mainly photoionised, we derive its ionic and *icf* total abundances. The derived values, with respect to H, are as follows: 1.39E-1, 7.37E-5, 3.74E-4, 1.74E-5 and 1.96E-6 for He, O, N, Ne and S, respectively. From the high He and N abundance obtained, K 4-47 is a typical Type I PN of the Galactic disk, while, somewhat in contradiction, its extreme oxygen deficiency is typical of Galactic halo PNe.

NGC 7009:

As one can see in Table 2, densities for the outer knots are very similar to those of the jets connecting them to the edge of the rim, with N_e(K$_1$) = 1,900 cm^{-3} and N_e(J$_1$)= 1,300 cm^{-3} and, on the opposite side, N_e(K$_4$) = 1,300 cm^{-3} and N_e(J$_2$) = 1,400 cm^{-3}. On the other hand, the rim has higher electron densities, namely N_e(R$_1$)= 5,500 cm^{-3} and N_e(R$_2$) = 5,900 cm^{-3}. As for the densities, the temperature estimators are appropriate for zones of low and medium to high excitation. The general trend of temperatures is that they are constant throughout the nebula, having an average value of T_e[O III] = 10,200 K

TABLE 2. Physical parameters and abundances of NGC 7009

$N_e(10^3 \mathrm{cm}^{-3})$ $T_e(10^3 \mathrm{K})$	K_1	R_1	R_2	K_4	**Whole nebula**
N_e[S II]	2	5.5	5.9	1.3	4
N_e[Cl III]	-	5.2	5.9	1.9	4.5
T_e[O III]	9.6	10	10.2	10.4	10.1
T_e[N II]	11	10.4	12.8	11.7	10.3
T_e[S II]	7.1	-	-	9.4	-
He/H (10^{-1})	1.0	1.0	1.1	0.95	1.1
O/H (10^{-4})	5.8	4.5	4.8	4.5	4.7
N/H (10^{-4})	3.8	0.7	1.8	2.5	1.7
Ne/H (10^{-4})	1.1	1.1	1.1	1.3	1.1
S/H (10^{-6})	0.13	6.1	4.9	9.3	8.3

and T_e[N II] = 11,100 K.

The empirical *icf* shown in Table 2 are homogeneous across the nebula, to within 9%, 17%, and 35% for He, O, and Ne and S, respectively. Nitrogen seems to be enhanced in the outer knots of NGC 7009 by a factor < 2, but this evidence is marginal considering the large range in the derived *icf*. The uncertainties intrinsic to the method are also rather large (Alexander & Balick 1997), but the present data seem to discard variations at the level found by Balick et al. (1994), namely outer knots overabundance by factors of 2 - 5.

PHOTOIONISATION MODELLING

The 1D-CLOUDY (Ferland et al. 1998) and the 3D-MOCASSIN (Ercolano et al. 2003; Ercolano 2005) photoionisation codes are used here in order to check whether or not the high T_e of the K 4-47's core and the N overabundance of the outer knots in NGC 7009 are real.

As input the photoionisation codes need information on the shape and intensity of the radiation from the ionizing source, the chemical composition and geometry of the nebula, as well as its density and size.

K 4-47: As mentioned before, the distance of K 4-47, and thus the size and the luminosity of the central star, are poorly known, but some measurements found in the literature lead to the values shown in the input parameters table. In Table 3 the L_* is the lower limit for the star luminosity, that comes from the *IRAS* spectral energy distribution (Tajitsu & Tamura 1998). The T_{eff} was obtained from the Core HeI and HeII nebular emission lines. A spherical geometry is adopted, with the size and density (which is constant) determined from the optical data (Corradi et al. 2000). Models with the much higher density derived from the radio data, consistent with the more compact core, of 0.25 arcsec (Aaquist & Kwok 1990)

were also tested.

With this set of parameters, we (Gonçalves et al. 2004) found partial agreement with the observed spectrum: most of the important lines for nebular diagnosis are well reproduced, with discrepancies of up to 35%. However, this model underestimates, by a factor of 3, the intensities of the auroral [O III] 4363Å and [N II] 5755Å lines, that are crucial for determining T_e. Note that for high density gas the auroral ([O III] 4363Å and [N II] 5755Å) to nebular ([O III] 5007Å and [N II] 6583Å) line ratios are indicators of density rather than of temperature (Gurzadyan 1970). Because of that, models with the much higher compact core density (from 72,000 cm^{-3} up to 10^5 cm^{-3}) are also calculated. With the latter model, the intensity of the auroral [O III] 4363Å and [N II] 5755Å can be reproduced, despite the fact that most of the other lines comes to be largely underestimated because of collisional quenching.

In short, none of the constant density models is able to account, simultaneously, for all optical emission lines in the Core. In particular, the [O III] 4363Å and [N II] 5755Å intensities are strongly underestimated if the nebular density is the one derived empirically from the [S II] lines. A model with a strong density stratification could possibly offer a solution to the problem. And, finally, if the strong density stratification of the Core is confirmed, the abundances quoted above, derived empirically, will not be valid anymore (Gonçalves et al. 2004).

TABLE 3. Input parameters

Inputs	K 4-47	NGC 7009
L_* ($L_\odot$)	550	3,136
T_{eff} (K)	120,000	80,000
N_e(cm^{-3})	1,900	Table 2*
D (kpc)	5.9	0.86
R_{out} (cm)	4.18E+16	3.88E+17
Abundances	Type-I PNe	Table 2†
Dust grains	ISM graphite+silicate	-

* We use the simplest possible 3D density distribution for NGC 7009, including an elliptical rim, surrounded by a spherical less opaque shell. At the polar tip of the rim, we connect the cylindrical jets that ended as disk-shaped knots. Densities in the different volumes (structures) match those in Table 2.
† Except that C/H=3.2E-4; N/H=2.0E-4 and Ar/H=1.2E-6

NGC 7009: When compared to K 4-47, the input parameters for the MOCASSIN modelling of NGC 7009 are considerably more reliable. As stated in the Introduction, its distance, central star effective temperature and luminosity are well constrained, and their values are given in Table 3. This table also shows the abundances adopted –mainly from Table 2 and Pottasch (2000)– and details about the geometry/density distribution assumed for this model. Note that: i) the emission of the spherical shell and the elliptical rim are combined, for easy comparison

with the long-slit spectrum; ii) the inner pair of knots are not being modelled, since they do not lie in the same direction of the outer knots and will not affect very much the ionisation structure in the outer knots; and iii) the jets are included in the model, because they transfer the radiation from the rim to the outer knots, but as they are very faint, their simulated spectra are not discussed.

A good agreement between the model and the dereddened intensities of the rim+shell and, even better, of the outer knots spectra is found (Gonçalves et al. 2005). All model predictions fall in between the data observed at the two sides of the nebula, or are within 10-30% of one of the two values. The temperature structure of the nebula is also well reproduced by this model, since the simulated figures of T_e[O III] and T_e[N II] for the rim, the knots and the whole nebula, all agree with the empirical values to better than 5%.

More importantly, concerning the ionisation structure of the simulated nebula, a relevant issue that should be emphasized here is the N/N^+ ratio being higher than the O/O^+ ratio by a factor of 1.39 in the knots, 1.66 in the rim and 1.61 in the total nebula. This result is at variance with the $N/N^+=O/O^+$ (Kingsburgh & Barlow 1994; Perinotto et al. 2004) generally assumed by the *icf* method, with the consequent errors on empirically derived total elemental abundances. Note also that only a small fraction (0.7%, 14% and 0.6% for rim, knots and whole nebula, respectively) of the total nitrogen in the nebula is in the form of N^0 and N^+. As only lines from these ions were observed (see Table 3 of Gonçalves et al. 2003), the nitrogen abundance determination is particularly uncertain. Therefore, *icf*s will be underestimated by the empirical scheme, for both components, rim and knots, but more so in the knots.

Finally, there is a strong dependence of the ionisation level on the geometry and density distribution of the gas, which makes the $(N^+/N)/(O^+/O)$ ratio extremely sensitive to the shape of the local radiation field. So that a realistic density distribution is essential to the modelling of a non-spherical PN, if one wants to get reliable information from spatially resolved observations (Gonçalves et al. 2005).

IN CONCLUSION

It should be finally noted that these (electron temperatures and chemical abundances) diagnosis are used not only to the analysis of PNe, but also to symbiotic systems, HII regions, and other ionised nebula, for which less constraints are generally available. For this reason it is of vital importance to verify the reliability of the present techniques for the determination of the basic PNe parameters.

REFERENCES

1. Aaquist, & Kwok, S. 1990, A&AS, 84, 229
2. Alexander J., & Balick B., 1997, AJ, 114, 713
3. Balick B., Rugers M., Terzian Y., Chengalur J. N., 1993, ApJ, 411, 778
4. Balick B., Perinotto M., Maccioni A., Alexander J., Terzian Y., & Hajian A. R., 1994, ApJ, 424, 800
5. Cahn, J. H., Kaler, J. B., & Stanghellini, L. 1992, A&AS, 94, 399
6. Corradi, R. L. M., Gonçalves, D. R., Villaver, E., Mampaso, A., Perinotto, M., Schwarz, H. E., & Zanin, C. 2000, ApJ, 535, 823
7. Ercolano B., Barlow M. J., Storey P. J., & Liu X.-W. 2003a, MNRAS, 340, 1136
8. Ercolano B., 2005, this proceedings
9. Ferland G. J., Korista K. T., Verner D. A., Ferguson J. W., Kingdon J. B., Verner E. M., 1998, PASP, 110, 761
10. Fernández R., Monteiro H., & Schwarz H. E., 2004, ApJ, 603, 595
11. Hyung S., & Aller L. H, 1995, MNRAS, 273, 958
12. Gonçalves D. R., Corradi R. L. M., & Mampaso A., 2001, ApJ, 547, 302
13. Gonçalves D. R., 2003, ASP Conf. Series, Vol. 313, 216
14. Gonçalves D. R., Corradi R. L. M., Mampaso A., & Perinotto M., 2003, ApJ, 597, 975
15. Gonçalves D. R., Mampaso A., Corradi R. L. M., Perinotto M., Riera A., López-Martín L., 2004, MNRAS, 355, 37
16. Gonçalves D. R., Ercolano B., Carnero A., Mampaso A., & Corradi R. L. M., 2005, MNRAS, in press
17. Gurzadyan, G. A.: 1970, 'Planetary Nebulae', Reidel, Dordrecht
18. Kingsburgh, R. L. & Barlow M. J., 1994, MNRAS, 271, 257
19. Lumsden, S. L., Puxley, P. J., & Hoare, M. G. 2001, MNRAS, 328, 419
20. Méndez R. H., Kudritzki R. P., & Herrero A., 1992, A&A, 260, 329
21. Perinotto M., Patriarchi P., Morbidelli L., & Scatarzi A., 2004b, MNRAS, 349, 793
22. Pottasch S. R., 2000, ASP Conf. Series, Vol. 199, 289
23. Reay N. K., & Atherton P.D., 1985, MNRAS, 215, 233
24. Tajitsu, A., & Tamura, S. 1998, AJ, 115, 1989
25. van de Steene, G. C., & Zijlstra, A. A. 1994, A&AS, 279, 521